

Measurement-based acceleration of optical computations

I. V. Vovchenko^{1,3}, A. A. Zyablovsky^{1,2,3}, A. A. Pukhov^{1,2}, E. S. Andrianov^{1,2,3}

¹*Moscow Center for Advanced Studies (MCAS), 20 Kulakova, Moscow 101000, Russia;*

²*Institute for Theoretical and Applied Electrodynamics, 13 Izhorskaya, Moscow 125412, Russia; and*

³*Dukhov Research Institute of Automatics (VNIIA), 22 Sushchevskaya, Moscow 127055, Russia;*

(Dated: January 13, 2026)

Analog coprocessors are intensively developing nowadays with the aim to optimize energy computations of neural networks. In this work we focus on the possibility of using detection of collective oscillations in optical systems for computational purposes. We show that in a system of coupled resonators, collective oscillations can be used to implement matrix-vector multiplication. The matrix is formed by the coupling constants between the resonators, and the input vector is formed by the initial occupancies of the involved modes. The frequency of the collective oscillations is growing with the number of the involved modes, similarly to Rabi oscillations. The time needed for their detection, i.e., averaging, decreases with an increase in the input vector dimension. We discuss the limitations imposed on parallel computation in the system by restriction of the allowed optical frequency band.

I. INTRODUCTION

Analog coprocessors [1–25] attract great attention in the field of applied science and are intensively developing nowadays. They are used in neural networks for acceleration of computations similarly to digital coprocessors [26–28]. Digital coprocessors are more precise than analog coprocessors [29, 30], while analog coprocessors are faster and more energy efficient [1–3, 13, 16, 17, 22–24]. Today, energy efficiency is considered an indispensable feature of a computational system [1, 2, 13]. This happens due to the extensive growth of data centers and their electricity consumption, which is evaluated to become of the order of electricity consumption of large countries in the following decade [3, 24, 31, 32].

Recently, optical coprocessors implementing linear operations in optical crossbar structures based either on waveguides and microring resonators [1, 4, 5] or meshes of interferometers [1, 6, 7] are actively investigated as candidates for energy efficiency improvement. Another approach is to use bosonic modes of free space to perform linear operations [9, 11, 12]. The width of the optical frequency band can be involved in computations to operate with tensors of higher dimension [2, 6, 10].

Important elements of the optical coprocessor are light detectors [33–37]. They deliver the result achieved in the optical computing scheme to the post-processing stage. The detectors are also used as non-linear elements to implement electro-optical activation functions [1, 2]. However, being non-linear elements, the detectors are not directly involved in the implementation of linear operations.

In turn, in the quantum computing measurement process, i.e., detection, is a principal building block of measurement-based quantum computers, which exploit one-way quantum processing of cluster states [38–43]. One can ask, could optical computing benefit from a possibility to use detectors not only for detection of the result of calculation but also as a part of calculation processes?

In quantum computations, detectors perform

quantum-mechanical averaging of certain operators [37]. In classical optics, detectors average oscillations of light field [33, 34, 37]. In turn, in systems consisting of many coupled modes, collective oscillations appear. An example of well-studied collective oscillations are Rabi oscillations appearing in systems of atoms coupled to light field modes [44–47]. The frequency of Rabi oscillations is growing with the number of involved atoms and photons in cavity [44–46, 48]. Then, it is expected that the frequencies of the collective oscillations appearing in the systems of many coupled modes should be similarly growing with the number of the involved modes. If so, the time that is required for detection, i.e., averaging, of such collective oscillations will decrease with an increase in the number of the involved modes. This can increase the speed of optical computing.

In this work we propose measurement-based acceleration of an optical coprocessor consisting of several resonators (the side resonators) coupled to a general one (the central resonator). We show that collective Rabi-like oscillations appear in the system. Being averaged, i.e., measured, occupancies of the central resonator's modes become proportional to the weighted initial occupancies of the side resonators' modes. We show that this can be used to implement matrix-vector multiplication. The matrix is formed by the coupling constants between the resonators' modes. The input vector is formed by the initial occupancies of the resonators' modes. The frequency of the collective Rabi-like oscillations is growing as a square root of the number of the involved modes. Hence, the time needed for the averaging, i.e., the computational time of the mentioned linear operation, is respectively decreasing with an increase in the input vector dimension. We discuss the limitations imposed on parallel computations by the restriction of the used optical frequency band. We show that the rate of parallel computations is primarily limited by the amount of cross-talk between modes of the side and central resonators that are non-resonant. We estimate the computational rate per one optical frequency as 10^{13} Hz.

II. THE MODEL

To describe the dynamics of N side resonators coupled to the central one, let consider the simplified model of one-mode resonators first, see Fig. 1. Further, we address the modes as side and central, respectively. The Hamiltonian of the system in the rotating wave approximation equals [37, 47, 49]

$$\hat{H} = \omega \hat{a}^\dagger \hat{a} + \sum_{k=1}^N \omega_b \hat{b}_k^\dagger \hat{b}_k + \sum_{k=1}^N \Omega_k (\hat{a}^\dagger \hat{b}_k + \hat{b}_k^\dagger \hat{a}). \quad (1)$$

Here ω is the frequency of the central mode, ω_b is the frequency of the side modes, Ω_k is the coupling constant between the k -th side mode and the central mode, $\hbar = 1$. Using Heisenberg representation, we get

$$\begin{aligned} \dot{\hat{a}}(t) &= -i\omega \hat{a}(t) - i \sum_{k=1}^N \Omega_k \hat{b}_k(t), \\ \dot{\hat{b}}_k(t) &= -i\omega_b \hat{b}_k(t) - i\Omega_k \hat{a}(t). \end{aligned} \quad (2)$$

Introducing operator $\hat{b}(t) = \sum_{k=1}^N \Omega_k \hat{b}_k(t) / \sum_{k=1}^N \Omega_k^2$, one can see that the dynamics of $\hat{a}(t)$ depends only on $\hat{b}(t)$, and the dynamics of $\hat{b}(t)$ depends only on $\hat{a}(t)$. Solving this set of two differential equations, one gets

$$\begin{aligned} \hat{a}(t) &= \left(\cos \Omega_R t - \frac{i\Delta/2}{\Omega_R} \sin \Omega_R t \right) \hat{a}(0) e^{-i\frac{\omega+\omega_b}{2}t} \\ &\quad - i \sin \Omega_R t \left(\frac{\vec{\Omega}}{\Omega_R}, \vec{\hat{b}}_0 \right) e^{-i\frac{\omega+\omega_b}{2}t}, \end{aligned} \quad (3)$$

Here $\vec{\hat{b}}_0 = (\hat{b}_1(0), \dots, \hat{b}_N(0))^T$, $\vec{\Omega} = (\Omega_1, \dots, \Omega_N)^T$, detuning is denoted as $\Delta = \omega - \omega_b$, $\Omega_R = \sqrt{\left(\frac{\Delta}{2}\right)^2 + (\vec{\Omega}, \vec{\Omega})}$, (\cdot, \cdot) denotes the usual Euclidean dot product. Thus,

$$\begin{aligned} \hat{a}^\dagger(t) \hat{a}(t) &= \left(\cos^2 \Omega_R t + \frac{(\Delta/2)^2}{\Omega_R^2} \sin^2 \Omega_R t \right) \hat{a}_0^\dagger \hat{a}_0 \\ &\quad + \sin^2 \Omega_R t \sum_{k=1}^N \frac{\Omega_k^2}{\Omega_R^2} \hat{b}_{k0}^\dagger \hat{b}_{k0} + \sin^2 \Omega_R t \sum_{k \neq q=1}^N \frac{\Omega_k \Omega_q}{\Omega_R^2} \hat{b}_{k0}^\dagger \hat{b}_{q0} \\ &\quad - i \left(\cos \Omega_R t + \frac{i\Delta/2}{\Omega_R} \sin \Omega_R t \right) \sin \Omega_R t \sum_{k=1}^N \frac{\Omega_k}{\Omega_R} \hat{a}_0^\dagger \hat{b}_{k0} \\ &\quad + i \left(\cos \Omega_R t - \frac{i\Delta/2}{\Omega_R} \sin \Omega_R t \right) \sin \Omega_R t \sum_{k=1}^N \frac{\Omega_k}{\Omega_R} \hat{b}_{k0}^\dagger \hat{a}_0. \end{aligned} \quad (4)$$

Here, $\hat{a}_0 = \hat{a}(0)$, $\hat{b}_{k0} = \hat{b}_k(0)$.

It is seen that collective oscillation at the frequency Ω_R influences the occupancy $\hat{a}^\dagger(t) \hat{a}(t)$. If $\Delta = 0$, $\Omega_R \sim \sqrt{N}$. Thus, the frequency of the collective oscillation Ω_R grows with an increase in the number of the modes involved in these collective oscillations, similarly to the way the

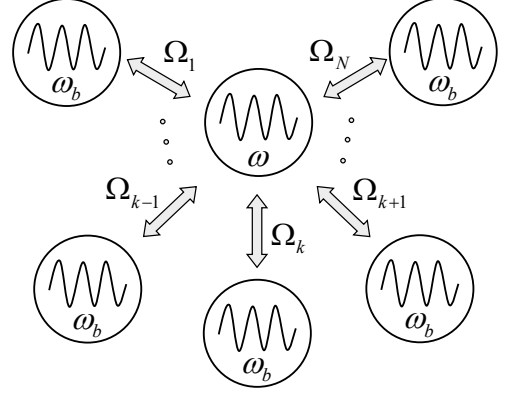


FIG. 1. Schematic representation of the system with Hamiltonian Eq. (1).

frequency of Rabi oscillations grows with an increase in the number of involved atoms or photons in cavity [44–46]. In view of this, further, we address this collective oscillation also as Rabi-like.

Detection of light averages its intensity over a time interval [33–37]. We can introduce the following function of time $\overline{\hat{a}^\dagger(t) \hat{a}(t)}_{t_0} \equiv \frac{1}{t} \int_0^{t_0} \hat{a}^\dagger(t') \hat{a}(t') dt'$ to describe the averaging of the central mode intensity. If $t = t_0 \gg 1/\Omega_R$, we get

$$\begin{aligned} \overline{\hat{a}^\dagger(t) \hat{a}(t)}_{t_0} &= \left(1 - \frac{(\vec{\Omega}, \vec{\Omega})}{2\Omega_R^2} \right) \hat{a}_0^\dagger \hat{a}_0 + \sum_{k=1}^N \frac{\Omega_k^2}{2\Omega_R^2} \hat{b}_{k0}^\dagger \hat{b}_{k0} \\ &\quad + \sum_{k=1}^N \frac{\Delta \Omega_k}{2\Omega_R^2} (\hat{a}_0^\dagger \hat{b}_{k0} + \hat{b}_{k0}^\dagger \hat{a}_0) + \sum_{k \neq q=1}^N \frac{\Omega_k \Omega_q}{2\Omega_R^2} \hat{b}_{k0}^\dagger \hat{b}_{q0}. \end{aligned} \quad (5)$$

Eq. (5) can be rewritten as

$$\begin{aligned} \overline{\hat{a}^\dagger(t) \hat{a}(t)}_{t_0} &= \hat{a}_0^\dagger \hat{a}_0 + \frac{(\vec{\Omega}, \vec{\Omega})}{2\Omega_R^2} \left(\sum_{k=1}^N \frac{\Omega_k^2}{(\vec{\Omega}, \vec{\Omega})} \hat{b}_{k0}^\dagger \hat{b}_{k0} - \hat{a}_0^\dagger \hat{a}_0 \right) \\ &\quad + \sum_{k=1}^N \frac{\Delta \Omega_k}{2\Omega_R^2} (\hat{a}_0^\dagger \hat{b}_{k0} + \hat{b}_{k0}^\dagger \hat{a}_0) + \sum_{k \neq q=1}^N \frac{\Omega_k \Omega_q}{2\Omega_R^2} \hat{b}_{k0}^\dagger \hat{b}_{q0}. \end{aligned} \quad (6)$$

Then, occupancy of the central mode averaged over time interval t_0 equals

$$\begin{aligned} \overline{\langle \hat{a}^\dagger \hat{a} \rangle}_{t_0} &= \langle \hat{a}^\dagger \hat{a} \rangle_0 + \frac{(\vec{\Omega}, \vec{\Omega})}{2\Omega_R^2} \left(\sum_{k=1}^N \frac{\Omega_k^2}{(\vec{\Omega}, \vec{\Omega})} \langle \hat{b}_k^\dagger \hat{b}_k \rangle_0 - \langle \hat{a}^\dagger \hat{a} \rangle_0 \right) \\ &\quad + \sum_{k=1}^N \frac{\Omega_k \Delta}{2\Omega_R^2} (\langle \hat{a}^\dagger \hat{b}_k \rangle_0 + \langle \hat{b}_k^\dagger \hat{a} \rangle_0) + \sum_{k \neq q=1}^N \frac{\Omega_k \Omega_q}{2\Omega_R^2} \langle \hat{b}_k^\dagger \hat{b}_q \rangle_0. \end{aligned} \quad (7)$$

Here, as previously for operators, index 0 denotes the value of the occupancy at $t = 0$. Let $\langle \hat{a}^\dagger \hat{a} \rangle_0 = 0$, $\text{Re}(\hat{a}^\dagger \hat{b}_k)_0 = 0$, and $\text{Re}(\hat{b}_k^\dagger \hat{b}_q)_0 \sim \delta_{kq}$, then

$$\overline{\langle \hat{a}^\dagger \hat{a} \rangle}_{t_0} = \frac{(\vec{\Omega}, \vec{\Omega})}{2\Omega_R^2} \sum_{k=1}^N \frac{\Omega_k^2}{(\vec{\Omega}, \vec{\Omega})} \langle \hat{b}_k^\dagger \hat{b}_k \rangle_0 \equiv \frac{(\vec{\Omega}, \vec{\Omega})}{2\Omega_R^2} \tilde{n}_b. \quad (8)$$

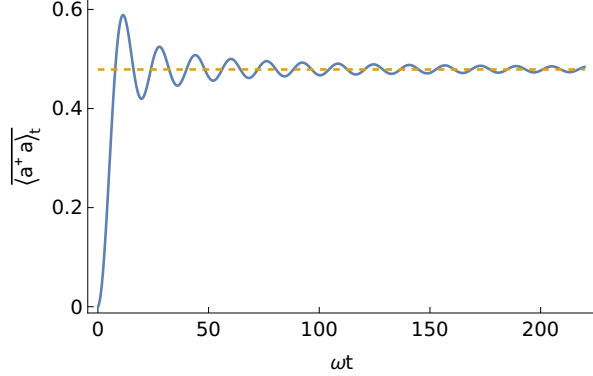


FIG. 2. The dynamics of $\overline{\langle \hat{a}^\dagger \hat{a} \rangle}_t$ (blue solid line) and $0.5\tilde{n}_b$ (orange dashed line). The parameters: $\omega = \omega_b = 1$, $N = 50$, Ω_k are set randomly between $5 \cdot 10^{-3}$ and $5 \cdot 10^{-2}$. Initial occupancies $\langle \hat{b}_k^\dagger \hat{b}_k \rangle_0$ are set randomly between 0.1 and 1, $\langle \hat{a}^\dagger \hat{a} \rangle_0 = 0$.

Here $\tilde{n}_b = \sum_{k=1}^N \Omega_k^2 \langle \hat{b}_k^\dagger \hat{b}_k \rangle_0 / (\vec{\Omega}, \vec{\Omega})$ is weighted initial occupancy of side modes. The weight coefficients are equal $\Omega_k^2 / (\vec{\Omega}, \vec{\Omega})$.

III. IMPLEMENTATION OF MATRIX-VECTOR MULTIPLICATION

Let $\Delta = 0$, then $\overline{\langle \hat{a}^\dagger \hat{a} \rangle}_{t_0} = 0.5\tilde{n}_b$. The dynamics of $\overline{\langle \hat{a}^\dagger \hat{a} \rangle}_t$ is presented in Fig. 2. It is seen that $\overline{\langle \hat{a}^\dagger \hat{a} \rangle}_t$ indeed tends to the value $0.5\tilde{n}_b$ while $t \rightarrow +\infty$. This requires $t_0 \approx 10\tau_R$, where $\tau_R = \Omega_R^{-1}$ (in Fig. 3 it is shown that for 3% precision of the convergence, the time $15\tau_R$ is required).

This dynamics of $\overline{\langle \hat{a}^\dagger \hat{a} \rangle}_t$ can be used for implementation of dot product. Indeed, let

$$\begin{aligned} \vec{A} &= (\Omega_1^2, \dots, \Omega_N^2)^T / (\vec{\Omega}, \vec{\Omega}), \\ \vec{B} &= (\langle \hat{b}_1^\dagger \hat{b}_1 \rangle_0, \dots, \langle \hat{b}_N^\dagger \hat{b}_N \rangle_0)^T, \\ \text{then } \overline{\langle \hat{a}^\dagger \hat{a} \rangle}_{t_0} &= 0.5(\vec{A}, \vec{B}). \end{aligned} \quad (9)$$

Thus, to implement the dot product of two positive vectors (one of which is normalized) in this system, one should tune normalized squares of coupling constants to form the first vector and excite the side modes occupancies to form the second vector. Then, the result of the dot product operation would be stored in the averaged value of the central mode occupancy.

If one gets several systems with Hamiltonian Eq. (1), he can implement multiple dot products in parallel or matrix-vector multiplication. (for the last one, occupancies of the side modes should be the same in different systems). With this scope, one can replicate the system or use the frequency domain of the resonators. Here we consider the second option.

Let consider N side resonators coupled to the central one. All resonators are similar and have M different modes. Let denote the frequency step in the resonators

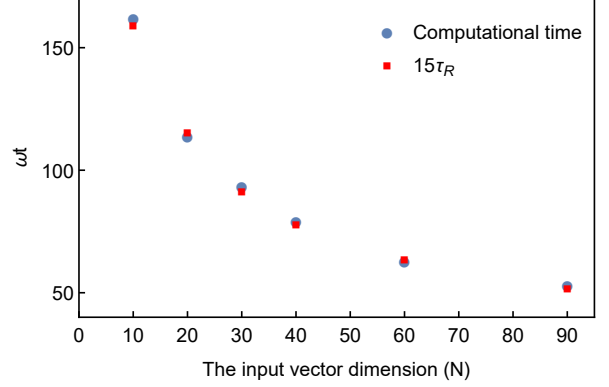


FIG. 3. The average value of the computational time providing 3% precision (blue circles) and $15\tau_R$ (red squares). The parameters are set similarly to Fig. 2.

as Δ_b . The model of one-mode resonators can be applied to this case too. For that, Δ_b should be sufficient to neglect both linear and non-linear cross-talk between non-resonant modes of side resonators via their coupling to the central resonator. If so, the model from the previous section can be applied to each mode of the central resonator independently. Hence, one can compute M independent dot products using this system. If the occupancies of the involved side resonators' modes are equal, one can realize matrix-vector multiplication

$$\begin{bmatrix} \overline{\langle \hat{a}^\dagger \hat{a} \rangle}_{t1} \\ \vdots \\ \overline{\langle \hat{a}^\dagger \hat{a} \rangle}_{tM} \end{bmatrix} \approx \frac{1}{2} \begin{bmatrix} p_{11} & \cdots & p_{1N} \\ \vdots & \ddots & \vdots \\ p_{M1} & \cdots & p_{MN} \end{bmatrix} \begin{bmatrix} \langle \hat{b}_1^\dagger \hat{b}_1 \rangle_0 \\ \vdots \\ \langle \hat{b}_N^\dagger \hat{b}_N \rangle_0 \end{bmatrix},$$

where $p_{mk} = (\Omega_k^{(m)})^2 / \sum_{q=1}^N (\Omega_q^{(m)})^2$. (10)

Here $\overline{\langle \hat{a}^\dagger \hat{a} \rangle}_{tm}$ is the averaged occupancy of the central resonator's mode resonant to the m -th mode of the side resonators, $1 \leq m \leq M$, $\Omega_k^{(m)}$ is the coupling constant between the m -th mode of the k -th side resonator and the central resonator's mode that is resonant to this mode of the side resonator. It is seen that the matrix involved in the computations is a stochastic matrix, i.e., a transition matrix (kernel) of a Markov process (Markov chain) [50–54]. Stochastic matrices are used in many sciences [53–58], including artificial intelligence and neural networks [53, 57–59].

Notably, the computational time that is of the order of τ_R decreases as $1/\sqrt{N}$ with an increase in the input vector dimension. Indeed, see Fig. 3. This happens due to the growth in frequency of the collective Rabi-like oscillations with an increase in N . This leads to the decrease in the time needed for the averaging, i.e., the computational time.

Also note that the factor $(\vec{\Omega}, \vec{\Omega})/2\Omega_R^2$ can be used to discriminate some of the inputs and outputs. With proper feedback loop design, this can help implementing the learning process used in neural networks [60–63].

IV. LIMITATION IMPOSED BY GEOMETRY AND RESTRICTED FREQUENCY BAND

The frequency band that can be used in computations is usually restricted by the frequency response of the detecting system [33–36]. For small matrices the influence of the finiteness of the frequency band can be neglected, as only several optical frequencies are involved in computations. Maximization of computational rate requires the usage of the whole frequency band and maximization of the number of computations per optical frequency. However, the maximization of computations per optical frequency leads to more intense non-resonant cross-talk between modes (see previous Section). This restricts the number of optical frequencies that can be used in parallel computations.

Let the frequency band that is used in computations be restricted by the width δ . Let $\Omega_{max}^{(\Delta)}$ be the maximal value of the non-resonant cross-talk coupling constant. We can use Eq. (8) to estimate the needed Δ_b . Indeed, the influence of non-resonant interaction on the averaged occupancy of the central resonator's modes decreases as Δ^{-2} with increase in detuning Δ , i.e., $(\vec{\Omega}, \vec{\Omega})/2\Omega_R^2 = 4(\vec{\Omega}, \vec{\Omega})/(\Delta^2 + 4(\vec{\Omega}, \vec{\Omega}))$. The $(\vec{\Omega}, \vec{\Omega})$ can be seen as the width of the Lorenz line. Then, to neglect the effect of cross-talk between non-resonant modes, the frequency step in resonators Δ_b should satisfy $\Delta_b \gg \sqrt{N}\Omega_{max}^{(\Delta)}$.

Hence, the maximal number of the optical frequencies that can be used in the computations equals $M = \delta/\sqrt{N}\Omega_{max}^{(\Delta)}$. Thus, the system can implement $N\delta/\sqrt{N}\Omega_{max}^{(\Delta)}$ elementary operations at once. The required time equals $\tau \sim \Omega_R^{-1} \sim N^{-1/2}\Omega_{max}^{-1}$, where $\Omega_{max} = \max_{k,m} \Omega_k^{(m)}$. Let introduce parameter $\alpha = \Omega_{max}^{(\Delta)}/\Omega_{max}$ which describes the ratio of non-resonant coupling to the resonant one. Then the rate of computations (number of elementary operations performed per second) can be estimated as $NM/\tau \sim \alpha^{-1}N\delta$.

One can see that the minimal rate of computations equals $N\delta$ (obviously $\alpha \leq 1$). It does not depend on coupling constants between the resonators. It increases linearly with an increase in the number of entries per optical frequency N and is inversely proportional to α . Thus, for fixed N , the maximization of the computational rate in a restricted frequency band is a problem of minimization of the cross-talk between non-resonant modes, i.e., minimization of α .

In turn, the maximal value of N is restricted in the used model. For the described model to be applicable, the time that is needed for the light to travel around the central resonator should be much less than the period of the collective Rabi-like oscillation. Then, $Nl_{max}/c \ll 1/\Omega_{max}\sqrt{N}$, i.e., $N \ll (c/\Omega_{max}l_{max})^{2/3}$, where l_{max} is the maximal coupling length between a side resonator and the central resonator. Let $l_{max} \sim 10^{-6}$ m, $\Omega_{max} \sim 10^9$ s $^{-1}$ (it should be greater than the dissipation rate, which is $\sim 10^7 \div 10^8$ s $^{-1}$ in resonators with high Q

factor [64–66]), then $N \ll 10^4$. Thus, at a single optical frequency, we get $N/\tau \ll N^{3/2}\Omega_{max} \ll c/l_{max} \sim 10^{14}$ Hz computational rate. Hence, the maximum value of the computational rate per optical frequency can be estimated as 10^{13} Hz.

Let the optical frequency band restricted by $1.5 \mu\text{m}$ and $0.4 \mu\text{m}$ be involved in the computations. Then, as for $\alpha \sim 1$ maximal value of $M \sim \delta/\sqrt{N}\Omega_{max}$, we can expect about 1000 optical frequencies computing in parallel, and the computational rate $N\delta \sim 10^{16}$ Hz in the system. Thus, the employment of parallel computations can increase the computational rate in the system by three orders of magnitude.

V. CONCLUSION AND DISCUSSION

In this work we describe measurement-based acceleration of an optical coprocessor. The considered coprocessor is based on side resonators coupled to a central resonator. We show that if the frequency step in the resonators is sufficient to neglect cross-talk between non-resonant modes, the averaged occupancies of the central resonator's modes are proportional to the weighted initial occupancies of the side resonators' modes. We show that this can be used to implement matrix-vector multiplications. The input vector is encoded in initial occupancies of the resonators' modes. The matrix is encoded by squares of coupling constants between the resonators' modes. The output vector is encoded in the averaged occupancies of the central resonator's modes.

The averaging, i.e., measurement, conducted by a detector levels out the collective Rabi-like oscillations that appear in the system. The frequency of the Rabi-like oscillations is growing as a square root of the number of the involved modes. Hence, the time that is needed for the averaging, i.e., the computational time, is decreasing as an inverse square root with an increase in the input vector dimension.

Finally, we discuss the limitations imposed on the parallel computations in the optical frequency band by the restriction of the optical frequency band that can be used. We show that it is impossible to maximize both the number of simultaneous computations per optical frequency and the number of the optical frequencies in parallel computations at the same time. We demonstrate that this happens due to cross-talk between non-resonant modes of the resonators. Thus, the computational rate in a restricted optical frequency band is proportional to the number of simultaneous computations per optical frequency and to the width of the used frequency band, and it is inversely proportional to the value of the non-resonant cross-talk. The computational rate per optical frequency can be estimated as 10^{13} Hz.

Note, we discuss the effect of collective Rabi-like oscillation on computations in an optical coprocessor. However, similar effects can be found in other frequency bands (microwave, for example) and systems of quasipar-

ticles obeying quadratic Hamiltonians, i.e., phonons [67–69], magnons [70–72], and plasmons [73–75].

Acknowledgment. A.A.Z. and E.S.A. acknowledge the support of the Foundation for the Advancement of Theoretical Physics and Mathematics BASIS.

[1] B. J. Shastri, A. N. Tait, T. Ferreira de Lima, W. H. Pernice, H. Bhaskaran, C. D. Wright, and P. R. Prucnal, Photonics for artificial intelligence and neuromorphic computing, *Nature Photonics* **15**, 102 (2021).

[2] O. Destrás, S. Le Beux, F. G. De Magalhaes, and G. Niculescu, Survey on activation functions for optical neural networks, *ACM Computing Surveys* **56**, 1 (2023).

[3] T. Ferreira De Lima, B. J. Shastri, A. N. Tait, M. A. Nahmias, and P. R. Prucnal, Progress in neuromorphic photonics, *Nanophotonics* **6**, 577 (2017).

[4] S. Ohno, R. Tang, K. Toprasertpong, S. Takagi, and M. Takenaka, Si microring resonator crossbar array for on-chip inference and training of the optical neural network, *Acs Photonics* **9**, 2614 (2022).

[5] D. Yi, Y. Wang, and H. K. Tsang, Multi-functional photonic processors using coherent network of micro-ring resonators, *APL Photonics* **6**, 100801 (2021).

[6] N. Youngblood, Coherent photonic crossbar arrays for large-scale matrix-matrix multiplication, *IEEE Journal of Selected Topics in Quantum Electronics* **29**, 1 (2022).

[7] G. Giamougiannis, A. Tsakyridis, Y. Ma, A. Totović, M. Moralis-Pegios, D. Lazovsky, and N. Pleros, A coherent photonic crossbar for scalable universal linear optics, *Journal of Lightwave Technology* **41**, 2425 (2023).

[8] S. Kovaios, I. Roumpos, A. Tsakyridis, M. Moralis-Pegios, D. Lazovsky, K. Vrysokinos, and N. Pleros, On-chip 1 tops hyperdimensional photonic tensor core using a wdm silicon photonic coherent crossbar, *J. Lightwave Technol.* **43**, 8799 (2025).

[9] D. Pierangeli, G. Marcucci, and C. Conti, Photonic extreme learning machine by free-space optical propagation, *Photonics Research* **9**, 1446 (2021).

[10] M. Miscuglio and V. J. Sorger, Photonic tensor cores for machine learning, *Applied Physics Reviews* **7** (2020).

[11] J. Hu, D. Mengu, D. C. Tzarouchis, B. Edwards, N. Engheta, and A. Ozcan, Diffractive optical computing in free space, *Nature Communications* **15**, 1525 (2024).

[12] X. Lin, Y. Rivenson, N. T. Yardimci, M. Veli, Y. Luo, M. Jarrahi, and A. Ozcan, All-optical machine learning using diffractive deep neural networks, *Science* **361**, 1004 (2018).

[13] N. C. Harris, J. Carolan, D. Bunandar, M. Prabhu, M. Hochberg, T. Baehr-Jones, M. L. Fanto, A. M. Smith, C. C. Tison, P. M. Alsing, *et al.*, Linear programmable nanophotonic processors, *Optica* **5**, 1623 (2018).

[14] W. Bogaerts, D. Pérez, J. Capmany, D. A. Miller, J. Poon, D. Englund, F. Morichetti, and A. Melloni, Programmable photonic circuits, *Nature* **586**, 207 (2020).

[15] J. Carolan, C. Harrold, C. Sparrow, E. Martín-López, N. J. Russell, J. W. Silverstone, P. J. Shadbolt, N. Matsuda, M. Oguma, M. Itoh, *et al.*, Universal linear optics, *Science* **349**, 711 (2015).

[16] M. Aifer, K. Donatella, M. H. Gordon, S. Duffield, T. Ahle, D. Simpson, G. Crooks, and P. J. Coles, Thermodynamic linear algebra, *Npj Unconventional Computing* **1**, 13 (2024).

[17] D. Melanson, M. Abu Khater, M. Aifer, K. Donatella, M. Hunter Gordon, T. Ahle, G. Crooks, A. J. Martinez, F. Sbahi, and P. J. Coles, Thermodynamic computing system for ai applications, *Nature Communications* **16**, 3757 (2025).

[18] A. Abbas, D. Sutter, C. Zoufal, A. Lucchi, A. Figalli, and S. Woerner, The power of quantum neural networks, *Nature Computational Science* **1**, 403 (2021).

[19] Z.-A. Jia, B. Yi, R. Zhai, Y.-C. Wu, G.-C. Guo, and G.-P. Guo, Quantum neural network states: A brief review of methods and applications, *Advanced Quantum Technologies* **2**, 1800077 (2019).

[20] N. Killoran, T. R. Bromley, J. M. Arrazola, M. Schulz, N. Quesada, and S. Lloyd, Continuous-variable quantum neural networks, *Physical Review Research* **1**, 033063 (2019).

[21] K.-H. Kim, S. Gaba, D. Wheeler, J. M. Cruz-Albrecht, T. Hussain, N. Srinivasa, and W. Lu, A functional hybrid memristor crossbar-array/cmos system for data storage and neuromorphic applications, *Nano letters* **12**, 389 (2012).

[22] Y. Li and K.-W. Ang, Hardware implementation of neuromorphic computing using large-scale memristor crossbar arrays, *Advanced Intelligent Systems* **3**, 2000137 (2021).

[23] S. Garg, J. Lou, A. Jain, Z. Guo, B. J. Shastri, and M. Nahmias, Dynamic precision analog computing for neural networks, *IEEE Journal of Selected Topics in Quantum Electronics* **29**, 1 (2023).

[24] Q. Xia and J. J. Yang, Memristive crossbar arrays for brain-inspired computing, *Nature materials* **18**, 309 (2019).

[25] D. Ma, J. Shen, Z. Gu, M. Zhang, X. Zhu, X. Xu, Q. Xu, Y. Shen, and G. Pan, Darwin: A neuromorphic hardware co-processor based on spiking neural networks, *Journal of systems architecture* **77**, 43 (2017).

[26] Y. Wu, J. Wang, K. Qian, Y. Liu, R. Guo, S. Hu, Q. Yu, T. Chen, Y. Liu, and L. Rong, An energy-efficient deep convolutional neural networks coprocessor for multi-object detection, *Microelectronics Journal* **98**, 104737 (2020).

[27] J. Lázaro, J. Arias, A. Astarloa, U. Bidarte, and A. Zuñaga, Hardware architecture for a general regression neural network coprocessor, *Neurocomputing* **71**, 78 (2007).

[28] A. Reuther, P. Michaleas, M. Jones, V. Gadepally, S. Samsi, and J. Kepner, Survey of machine learning accelerators, in *2020 IEEE high performance extreme computing conference (HPEC)* (IEEE, 2020) pp. 1–12.

[29] P. Jawandhiya, Hardware design for machine learning, *Int. J. Artif. Intell. Appl.* **9**, 63 (2018).

[30] F. M. Dias, A. Antunes, and A. M. Mota, Commercial hardware for artificial neural networks: A survey, *IFAC Proceedings Volumes* **36**, 189 (2003).

[31] A. Shehabi, A. Hubbard, A. Newkirk, N. Lei, M. A. B. Siddik, B. Holecek, J. Koomey, E. Masanet, D. Sartor, *et al.*, *2024 united states data center energy usage report*

(Lawrence Berkeley National Laboratory, Berkeley, California, 2024).

[32] IEA, *World energy Outlook 2023* (IEA, Paris, 2023).

[33] B. Nabet, *Photodetectors: Materials, Devices and Applications* (Woodhead publishing, 2023).

[34] G. Rieke, *Detection of Light: from the Ultraviolet to the Submillimeter* (Cambridge University Press, 2003).

[35] S. Gundacker, E. Auffray, N. Di Vara, B. Frisch, H. Hillemanns, P. Jarron, B. Lang, T. Meyer, S. Mosquera-Vazquez, E. Vauthey, *et al.*, Sipm time resolution: From single photon to saturation, Nuclear Instruments and Methods in Physics Research Section A: Accelerators, Spectrometers, Detectors and Associated Equipment **718**, 569 (2013).

[36] S. Seifert, H. T. Van Dam, R. Vinke, P. Dendooven, H. Lohner, F. J. Beekman, and D. R. Schaart, A comprehensive model to predict the timing resolution of sipm-based scintillation detectors: theory and experimental validation, IEEE Transactions on nuclear science **59**, 190 (2012).

[37] H. Carmichael, *An open systems approach to quantum optics: lectures presented at the Université Libre de Bruxelles, October 28 to November 4, 1991*, Vol. 18 (Springer Science & Business Media, 2009).

[38] R. Raussendorf and H. J. Briegel, A one-way quantum computer, Physical review letters **86**, 5188 (2001).

[39] H. J. Briegel, D. E. Browne, W. Dür, R. Raussendorf, and M. Van den Nest, Measurement-based quantum computation, Nature Physics **5**, 19 (2009).

[40] R. Prevedel, P. Walther, F. Tiefenbacher, P. Böhi, R. Kaltenbaek, T. Jennewein, and A. Zeilinger, High-speed linear optics quantum computing using active feed-forward, Nature **445**, 65 (2007).

[41] M. Kues, C. Reimer, J. M. Lukens, W. J. Munro, A. M. Weiner, D. J. Moss, and R. Morandotti, Quantum optical microcombs, Nature Photonics **13**, 170 (2019).

[42] C. Reimer, S. Sciara, P. Roztocki, M. Islam, L. Romero Cortés, Y. Zhang, B. Fischer, S. Loranger, R. Kashyap, A. Cino, *et al.*, High-dimensional one-way quantum processing implemented on d-level cluster states, Nature Physics **15**, 148 (2019).

[43] Y. Wang, Z. Hu, B. C. Sanders, and S. Kais, Qudits and high-dimensional quantum computing, Frontiers in Physics **8**, 589504 (2020).

[44] M. O. Scully and M. S. Zubairy, *Quantum optics* (Cambridge university press, 1997).

[45] S. Barnett and P. M. Radmore, *Methods in theoretical quantum optics*, Vol. 15 (Oxford University Press, 2002).

[46] A. Rahimi-Iman, *Polariton physics*, Vol. 229 (Springer, 2020).

[47] A. A. Lisyansky, E. S. Andrianov, A. P. Vinogradov, and V. Y. Shishkov, *Quantum Optics of Light Scattering* (Springer, 2024).

[48] J. Fregoni, F. J. Garcia-Vidal, and J. Feist, Theoretical challenges in polaritonic chemistry, ACS photonics **9**, 1096 (2022).

[49] H.-P. Breuer and F. Petruccione, *The theory of open quantum systems* (Oxford University Press, USA, 2002).

[50] J. R. Norris, *Markov chains*, Vol. 2 (Cambridge university press, 1998).

[51] R. Douc, E. Moulines, P. Priouret, and P. Soulier, *Markov chains*, Vol. 4 (Springer, 2018).

[52] D. Freedman, *Markov chains* (Springer Science & Business Media, 2012).

[53] J. I. Agbinya, *Applied data analytics-principles and applications* (CRC Press, 2022).

[54] R. L. Tweedie, Markov chains: Structure and applications, Handbook of statistics **19**, 817 (2001).

[55] S. Brooks, Markov chain monte carlo method and its application, Journal of the royal statistical society: series D (the Statistician) **47**, 69 (1998).

[56] A. Tamir, *Applications of Markov chains in chemical engineering* (Elsevier, 1998).

[57] O. Sigaud and O. Buffet, *Markov decision processes in artificial intelligence* (John Wiley & Sons, 2013).

[58] V. Torra, M. Taha, and G. Navarro-Arribas, The space of models in machine learning: using markov chains to model transitions, Progress in Artificial Intelligence **10**, 321 (2021).

[59] S. Pardo-Guerra, J. J. Li, K. Basu, and G. A. Silva, Neural networks and markov categories, AppliedMath **5**, 93 (2025).

[60] H. Abdi, D. Valentin, and B. Edelman, *Neural networks* (Sage, 1999).

[61] K. Gurney, *An introduction to neural networks* (CRC press, 2018).

[62] M. Islam, G. Chen, and S. Jin, An overview of neural network, American Journal of Neural Networks and Applications **5**, 7 (2019).

[63] B. Müller, J. Reinhardt, and M. T. Strickland, *Neural networks: an introduction* (Springer Science & Business Media, 2012).

[64] L. Wu, H. Wang, Q. Yang, Q.-x. Ji, B. Shen, C. Bao, M. Gao, and K. Vahala, Greater than one billion q factor for on-chip microresonators, Optics Letters **45**, 5129 (2020).

[65] A. Shitikov, I. Bilenko, N. Kondratiev, V. Lobanov, A. Markosyan, and M. Gorodetsky, Billion q-factor in silicon wgm resonators, Optica **5**, 1525 (2018).

[66] D.-G. Kim, S. Han, J. Hwang, I. H. Do, D. Jeong, J.-H. Lim, Y.-H. Lee, M. Choi, Y.-H. Lee, D.-Y. Choi, *et al.*, Universal light-guiding geometry for on-chip resonators having extremely high q-factor, Nature communications **11**, 5933 (2020).

[67] S. Minarik and V. Labas, Hamiltonian of acoustic phonons in inhomogeneous solids, Journal of Modern Physics , 373 (2013).

[68] R. Zaitsev, *Introduction to modern statistical physics : a set of lectures* (URSS, 2008).

[69] P. Scherer and S. F. Fischer, On the theory of vibronic structure of linear aggregates. application to pseudoiso-cyanin (pic), Chemical physics **86**, 269 (1984).

[70] H. Yuan and X. Wang, Magnon-photon coupling in antiferromagnets, Applied Physics Letters **110**, 082403 (2017).

[71] C. Kittel, *Quantum Theory of Solids* (Wiley, 1991).

[72] P. A. McClarty, Topological magnons: A review, Annual Review of Condensed Matter Physics **13**, 171 (2022).

[73] M. S. Tame, K. McEnergy, S. Özdemir, J. Lee, S. A. Maier, and M. Kim, Quantum plasmonics, Nature Physics **9**, 329 (2013).

[74] C. A. Downing and G. Weick, Topological collective plasmons in bipartite chains of metallic nanoparticles, Physical Review B **95**, 125426 (2017).

[75] S.-A. Biehs and G. S. Agarwal, Dynamical quantum theory of heat transfer between plasmonic nanosystems, Journal of the Optical Society of America B **30**, 700

(2013).